Evaluation of the Cylinder Implant Thread Height and Width: A 3-dimensional Finite Element Analysis

Liang Kong, DDSc[1]/Kaijin Hu, DDSc[2]/Dehua Li, DDSc[3]/Yingliang Song, DDSc[4]/
Jin Yang[5]/Ziyan Wu[6]/Baolin Liu, DDSc[2]

Purpose: *To evaluate continuous and simultaneous variations of thread height and width for an experimental screw-type implant.* ***Materials and Methods:*** *A finite element model of an implant with a V-shaped thread was created. The range of thread height was set at 0.20 to 0.60 mm, and the range of thread width was set at 0.10 to 0.40 mm. Forces of 100 N and 50 N were applied along the implant axis (AX) and an angle of 45 degrees in a buccolingual direction (45-degree BL), respectively. The maximum von Mises stresses in jawbone were evaluated, and the sensitivity of the stress in jawbone to the variables was also evaluated.* ***Results:*** *Under AX load, the maximum von Mises stresses in cortical and cancellous bones increased by 4.3% and 63.0%, respectively, as thread parameters changed. Under 45-degree BL load, maximum von Mises stresses in cortical and cancellous bones increased by 19.3% and 118.0%, respectively. When thread height was from 0.34 to 0.50 mm and thread width was 0.18 to 0.30 mm, the tangent slope of the maximum von Mises stress response curve ranged from −1 to 1. The variation of the maximum von Mises stresses in jawbone was more sensitive to thread height than to thread width.* ***Conclusions:*** *Stress in cancellous bone is more likely to be influenced by thread parameters than stress in cortical bone. A 45-degree BL force is more likely to be influenced by thread parameters than an axial force. A thread height of 0.34 to 0.50 mm and a thread width of 0.18 to 0.30 mm is optimal from a biomechanical point of view. In the design of a screw-type implant, thread height is more important than thread width for the reduction of stress within the bone.* Int J Oral Maxillofac Implants 2008;23:65–74

Key words: *3-dimensional finite element analysis, dental implant, optimized thread design, stress*

A crucial factor that affects the outcome of implant treatment is the way occlusal forces are transferred to the bone-implant interface via the implant and the superstructure. The interface must tolerate occlusal forces without adverse tissue response.[1] In natural teeth, the periodontal ligament acts as an intermediate cushion element to buffer occlusal forces. However, in the case of osseointegrated dental implants, occlusal loads are transmitted directly to the surrounding bone. This could cause microfracture at the bone-implant interface, fracture of the implant, loosening of the components of implant system, or unwanted bone resorption.

Several researchers have attempted to minimize crestal bone resorption by increasing the bone-implant contact and therefore reducing stress at the cortical alveolar crest. Attempts to increase bone-implant contact have focused on increasing the diameter and/or length of the implant, altering the shape and characteristics of the implant surface, or altering the implant design/shape.[2–9] Thread configuration is an important consideration in biomechanical optimization of the dental implant. Threads are

[1]Lecturer, Department of Oral and Maxillofacial Surgery, School of Stomatology, Fourth Military Medical University, Xi'an, China.
[2]Professor, Department of Oral and Maxillofacial Surgery, School of Stomatology, Fourth Military Medical University, Xi'an, China.
[3]Professor, Department of Implantology, School of Stomatology, Fourth Military Medical University, Xi'an, China.
[4]Associate Professor, Department of Implantology, School of Stomatology, Fourth Military Medical University, Xi'an, China.
[5]Lecturer, Department of Civil Engineering, Northwestern Polytechnical University, Xi'an, China.
[6]Associate Professor, Northwestern Polytechnical University, Xi'an, China.

Correspondence to: Dr Baolin Liu, Department of Oral and Maxillofacial Surgery, School of Stomatology, Fourth Military Medical University, 145 Changlexi Street, Xi'an, 710032, Shaanxi, PRC.
E-mail: baolin@fmmu.edu.cn, implant@fmmu.edu.cn

used to maximize initial contact, improve initial stability, increase implant surface area,[10] and help dissipate interfacial stress.[11] Thread depth, thread thickness, thread face angle, thread pitch, and thread helix angle are some of the characteristics that determine the functional thread surface and affect the biomechanical load distribution of the implant.[12]

Bumgardner et al reported that the face angle of the thread can change the direction of load from the prosthesis to a different direction at the bone.[13] The original Brånemark screw, introduced in 1965, had a V-shaped thread pattern and was to be placed into a threaded osteotomy.[14] For a dental implant under axial loading, a V-thread is comparable to a buttress thread when the face angle is similar.[12] In studies of retrieved dental implants, it was found that bone defects tended to be located at the end of each thread.[15] A square thread design (as opposed to the standard V-shaped or buttress thread) was suggested to reduce the shear component of force by transferring axial load from the prosthesis to the implant body to compress the bone.[16]

To enhance clinical success, it is necessary to understand how the stress concentration on implants is affected by the shape, width, and height of thread. The use of the finite element method (FEM) in implant biomechanics analysis offers many advantages over other methods in simulating the complexity of clinical situations. It allows researchers to predict stress distribution between implants and cortical or cancellous bone.[12,13] Many previous finite element studies have examined the effect of implant design parameters discretely and independently,[13,17] with implant thread parameter analyses most often based on 2-dimensional simulation.[8,15,18,19] This method was not accurate, and some important information about the implant design parameters was lost.

Despite the apparent importance of the implant thread in the transfer of force to the bone, no controlled clinical studies comparing the thread parameters are available. The main aim of the present study was to perform 3-dimensional (3D) finite element analyses on continuous and simultaneous variations of implant thread height and width to find optimal thread parameters under idealized axial and buccolingual loads to minimize peak stress in the jawbone.

MATERIALS AND METHODS

The study was performed by means of 3D finite element analysis.[20] The materials were assumed to be linearly elastic[21]; no separations were allowed between the bone and implant, and there was no plastic deformation of the models.

3D Model Design

A mandibular segment with an implant and a superstructure were modeled on a personal computer using a 3D modeling program (Pro/E Wildfire, Parametric Technology, Needham, MA). The bone was modeled as cancellous core surrounded by a 1.3-mm cortical layer.[22,23]. The dimensions of the bone segment are shown in Fig 1. The geometry of the 13-mm solid-thread implant (Nobel Biocare, Göteborg, Sweden) was used as a reference to model a cylindric implant and a 5-mm-high solid abutment which were modeled as a single unit for simplification, as shown in Fig 1. The box-shaped void in the implant body below the abutment screw was also modeled. A porcelain superstructure with an occlusal thickness of 2 mm was applied over the titanium abutment (Fig 1). Thread parameters are shown in Fig 2. The height of thread (H) and width of thread end (W) were set as the input variables. H ranged from 0.20 mm to 0.60 mm, and W ranged from 0.10 mm to 0.40 mm. Although thread pitch could affect the stress distribution, traditionally, implant manufacturers have provided implant systems with a constant pitch. It was assumed that the first thread was placed level with cortical bone-cancellous bone junction. The study is primarily concerned with the stress distribution of the jawbone, which is affected by simultaneous changes of the thread height and width. All the models were meshed using Ansys Workbench 9.0 (Ansys, Canonsburg, PA).

Material Properties

All materials used in the models were considered isotropic, homogeneous, and linearly elastic. The elastic properties were taken from the literature, as shown in Table 1.

Interface Conditions

The condition of osseointegration was simulated. The implant was rigidly anchored in the bone model along its entire interface. The same type of contact was provided at the prosthesis-abutment interface.

Elements and Nodes

The models were meshed with 10-node tetrahedron and 20-node hexahedron elements (Fig 3). A refinement mesh was generated around the implant. The same meshing method was used for all models. Models were composed of an average of 31,000 elements and 52,000 nodes.

Constraints and Loads

Models were constrained in all directions at the nodes at the mesial and distal edges of the bone. Since this study was aimed at investigating effects on

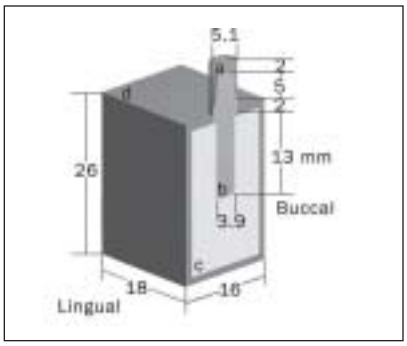

Fig 1 Cross-sectional view of the symmetry plane of 1 model. a = superstructure; b = implant and abutment; c = cancellous bone; d = cortical bone.

Fig 2 Schematic representation of the screw parameters: Zoom view of screw *(right)*. H = height, W = width.

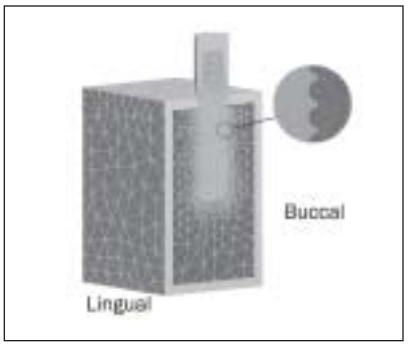

Fig 3 Cross-sectional view of a meshed model.

bone effects to loads within physiologic limits, rather than overloads, forces of 100 N and 50 N were applied along the axis of the implant (AX) and at an angle of 45 degrees in a buccolingual direction (45 degrees BL) to the middle point in the center of the superstructure.[22,23] Analysis of each load was performed using the Ansys Workbench software program. The maximum von Mises stresses (maximum equivalent stress, abbreviated Max EQV stress) in the cortical and cancellous bones were set as output variables to evaluate the effect of different designs on the jawbone. The sensitivity of the jawbone to the height and width was also evaluated.

RESULTS

The Max EQV stresses in jawbone are shown as response charts, with different colors for each range (Figs 4 to 7). The response curves of one variable to the Max EQV stress are shown in Table 2 when the other variable is equal to the median. The samplings of this research are listed in Table 3, and the stress distributions of the cortical and cancellous bone are shown in Fig 8. Because the sensitivities of the jawbone to the variables were similar in range, a sensitivity chart for a thread height of 0.40 mm and a thread width of 0.25 mm is shown in Fig 9. All the figures were drawn by Ansys Workbench DesignXplorer module automatically.

When a straight line is tangent to a curve, the slope rate of the straight line shows the changing frequency of the curve. When the slope rate ranges from –1 to 1, it indicates the slight changing of the Max EQV stress in response to the changing variables (Fig 10). If the Max EQV stress reaches the minimal value, the optimum thread parameters should be in this range.

Table 1 Elastic Properties of Materials in the 3D FEM Models

Material	Young's modulus (GPa)	Poisson's ratio	References
Cortical bone	14	0.30	41
Cancellous bone	1.37	0.30	42
Titanium	110	0.35	43
Porcelain	68.9	0.28	44

Stress Distribution

In all loading situations, the highest stress in the bone, as a whole, was concentrated in the cortical bone around the implant. Because of a great difference between the stress values in the cortical and cancellous bone, the stress distributions in these bone regions are shown separately.

In all the models under AX load, the Max EQV stress of the cortical bone was observed around the implant neck. High stress surrounded the implant neck like a ring. The distribution of the EQV stress was similar for all models (Fig 10a). Under 45-degree BL load, the highest EQV stress was observed buccally and lingually near the implant neck in all models. The distribution of the EQV stress was similar for all models (Fig 10b).

In all the models under AX load, the highest EQV stress of the cancellous bone was observed at the implant apex, but Max EQV stress was much lower in cancellous bone than in cortical bone (Fig 10c). Under 45-degree BL load, the highest EQV stress occurred near the cortical plates on the buccal and lingual sides. The EQV stress was much higher on the buccal sides than on the lingual sides for all models (Fig 10d).

AX Load in Cortical Bone

Max EQV stress in cortical bone increased as thread height decreased. It ranged from 3.70 to 3.86 MPa

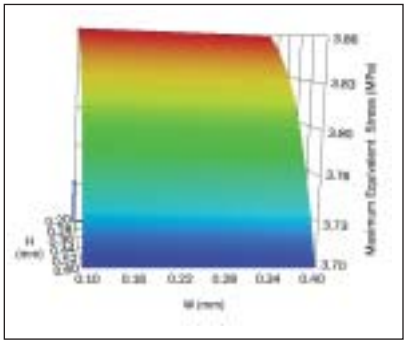

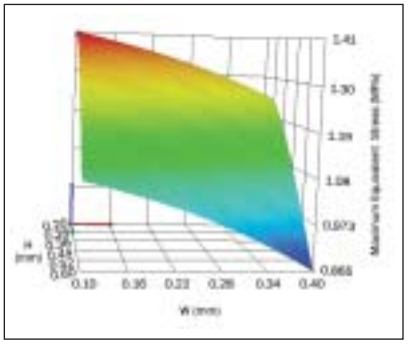

Fig 4 Under AX load, response surface nephogram of the relationship between various height and width combinations and maximum von Mises stresses in cortical bone.

Fig 5 Under AX load, response surface nephogram of the relationship between various height and width combinations and maximum von Mises stresses in cancellous bone.

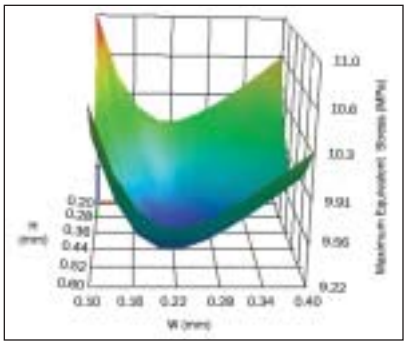

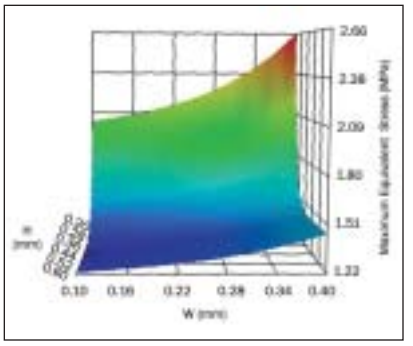

Fig 6 Under 45-degree buccolingual load, response surface nephogram of the relationship between various height and width combinations to maximum von Mises stresses in cortical bone.

Fig 7 Under 45-degree buccolingual load, response surface nephogram of the relationship between various height and width combinations to maximum von Mises stresses in cancellous bone.

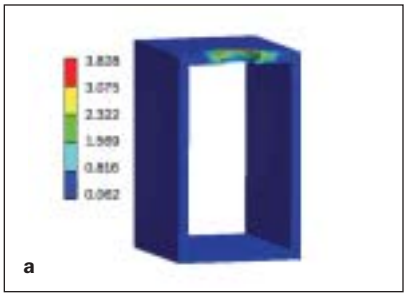

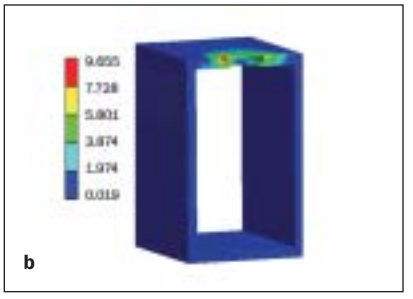

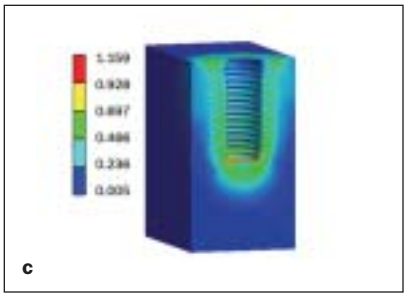

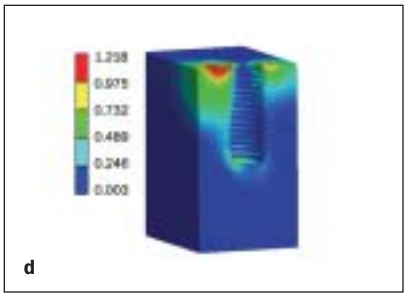

Fig 8 Cross-sectional view illustrating EQV stress distribution in the jawbone (H = 0.40 mm, W = 0.40 mm). *(a)* EQV stress distribution in cortical bone under AX load. *(b)* EQV stress distribution in cortical bone under 45-degree BL load. *(c)* EQV stress distribution in cancellous bone under AX load. *(d)* EQV stress distribution in cancellous bone under 45-degree BL load.

and increased by 4.3% (Fig 4). The tangent slope of the rate of response curve reached about –1 (Table 2). Thread width showed little effect on Max EQV stress in cortical bone (Fig 8a).

AX Load in Cancellous Bone

Max EQV stress in cancellous bone increased as thread height and width decreased. It ranged from 0.865 to 1.41 MPa and increased by 63.0% (Fig 5). When thread height exceeded 0.34 mm, the tangent slope of the response curve ranged from –1 to 0. The tangent slope of the response curve reached about –1 when thread width ranged from 0.10 to 0.40 mm (Table 2). Thread height affected the Max EQV stress of cancellous bone more than width did (Fig 8b).

Table 2 Response Curve of Univariate Analysis to Max EQV Stresses in Jawbone

	AX load		45-degree BL load	
Max EQV stress (MPa)	**Cortical bone**	**Cancellous bone**	**Cortical bone**	**Cancellous bone**
H (0.2–0.6 mm) W = 0.25 mm	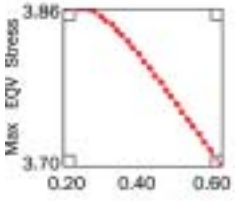	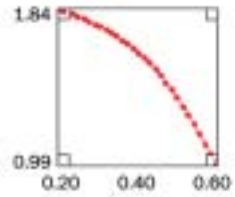	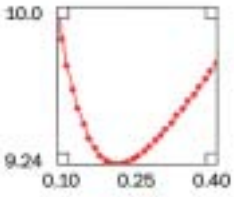	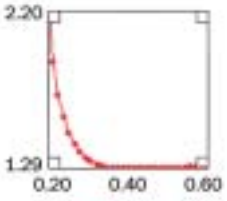
Increased percentage	4.32%	85.86%	8.23%	70.54%
W (0.1–0.4 mm) H = 0.4 mm	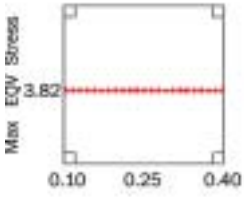	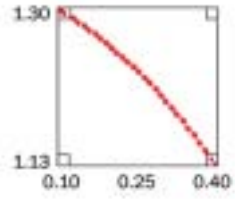	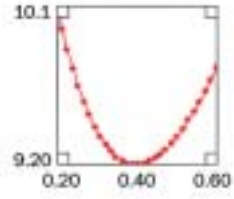	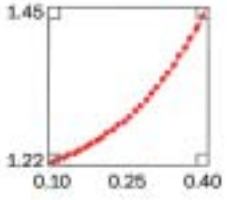
Increased percentage	0.00%	15.04%	9.78%	18.85%

Increased percentage = $(Stress_{Max}–Stress_{Min})/Stress_{Min} * 100\%$

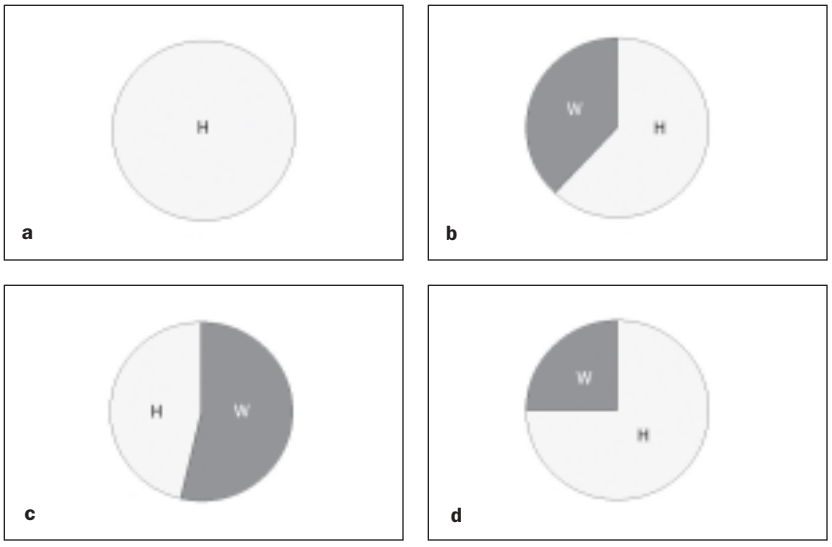

Fig 9 The sensitivity analysis of maximum von Mises stresses in jaw bone to variable thread height (H) and width (W). *(a)* Under AX load, maximum von Mises stresses in cortical bone to variable. *(b)* Under AX load, maximum von Mises stresses in cancellous bone to variable. *(c)* Under 45-degree BL load, maximum von Mises stresses in cortical bone to variable. *(d)* Under 45-degree BL load, maximum von Mises stresses in cancellous bone to variable.

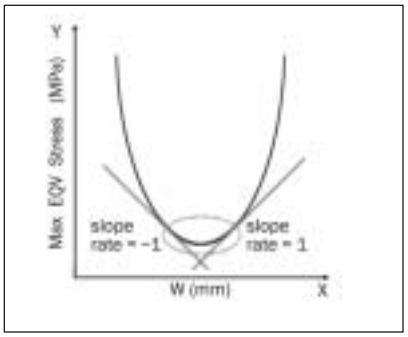

Fig 10 Chart of the optimum selection of the curve: Slight changing and minimal value of the curve.

Table 3 Max EQV Stresses in Jawbone of the Samplings (MPa)

			Max EQV stress in cortical bone		Max EQV stress in cancellous bone	
	H (mm)	W (mm)	AX load	45-degree BL load	AX load	45-degree BL load
1	0.40	0.25	3.8714	9.2636	1.2216	1.4235
2	0.40	0.10	3.8316	10.130	1.3330	1.2249
3	0.40	0.40	3.8280	9.7365	1.1585	1.5152
4	0.20	0.25	3.8956	10.035	1.3417	2.2095
5	0.60	0.25	3.6820	9.6676	1.0454	1.1826
6	0.25858	0.14393	3.8073	9.9529	1.3754	1.4207
7	0.25858	0.35607	3.7919	9.8857	1.2594	1.5799
8	0.54142	0.14393	3.7928	9.7169	1.2564	1.0772
9	0.54142	0.35607	3.7034	10.041	0.9440	1.3325

45-degree BL Load in Cortical Bone

Higher Max EQV stresses were found in cortical bone when thread height and width were very large and/or very small. Max EQV stress in cortical bone ranged from 9.22 to 11.0 MPa and increased by 19.3% (Fig 6). When height ranged from 0.33 mm to 0.50 mm or width changed from 0.18 to 0.30 mm, the tangent slope rate of response curve ranged from –1 to 1 (Table 2). Thread height and width affected Max EQV stress in cortical bone similarly (Fig 8c).

45-degree BL Load in Cancellous Bone

Max EQV stress in cancellous bone increased as thread height decreased and thread width increased. It ranged from 0.865 MPa to 1.41 MPa and increased by 118.0% (Fig 7). When thread height exceeded 0.30 mm, the tangent slope of the response curve ranged from –1 to 0, and when thread width was less than 0.30 mm, the tangent slope of the response curve ranged from 0 to 1 (Table 2). Thread height affected the Max EQV stress of cancellous bone more than thread width did (Fig 8d).

DISCUSSION

The aim of the present study was to determine the effect of the variations of the thread height and width upon stress within the bone. For this reason it was assumed that all the parameters of the models were identical except the thread height and width. This made it possible to compare implants of different thread heights and widths. The Workbench Simulation module was used to define the environmental loading conditions of the model. An optimized implant parameter design was selected by the DesignXplorer module.

Ansys Workbench DesignXplorer

There were 3 key points in this new FEM: self-adapting 3D model assembly, bidirectional parameter transmittal, and variables settings. In this study, "self-adapting 3D model assembly" means all the models were rebuilt based on implant parameters. In other words, the parameters of models (cortical bone and cancellous bone) changed with the parameters (thread height and width) of the implant, varying automatically. "Bidirectional parameter transmittal" means computer-aided design (CAD) software (Pro/E and Ansys Workbench in this study) could transmit the model's parameters seamlessly. Variables included input variables (thread height and width) and output variables (Max EQV stresses in cortical and cancellous bones). Thus, only 1 assembled model was needed, and the time of model regeneration and the solving process were shortened.

Furthermore, the result could be shown as a response surface (Figs 4 to 7), a response curve (Table 2), and a sensitivity chart (Fig 10). Other input and output parameters could also be evaluated, either simultaneously or in future studies, such as implant diameter, implant length, superstructure thickness, elastic properties, strains in jawbone, shear strains in jawbone, and loading forces.

In this study, 9 analyses were performed to construct the response surfaces (Figs 4 to 7). In the DesignXplorer environment, samplings generation is based on the Latin Hybercube Sampling (LHS) technique. The LHS technique is a more advanced and efficient form of Monte Carlo Simulation methods. The only difference between LHS and the Direct Monte Carlo Sampling technique is that LHS has a sample "memory," meaning it avoids repeating samples that have been evaluated before (ie, it avoids clustering samples). It also forces the tails of a distrib-

ution to participate in the sampling process. Generally, the LHS technique requires 20% to 40% fewer simulation loops than the Direct Monte Carlo Simulation technique to deliver the same results with the same accuracy.

Ansys DesignXplorer can also provide sensitivity charts to demonstrate the impact of the input parameters on the response and derived parameters. The sensitivity charts are "single-parameter sensitivities." This means that DesignXplorer calculates the change of the output based on the change of each input independently at the current value of each input parameter. The larger the change of the output, the more significant the input parameter that was varied. As such, single-parameter sensitivities are local sensitivities. Changing the input parameter values updates the sensitivities. When the input parameter (height and width) changed, sensitivity charts changed little in this study. So when 1 of the input parameters was set (H = 0.40 mm; W = 0.25 mm), the corresponding sensitivity chart was selected to show the full range of the output sensitivity to input (Fig 8).

In contrast to the discrete variations of previous finite element studies,[8,15,19] continuous variations of the 2 investigated factors were shown as response surfaces and curves in this study. More accurate results, better visualization of results, and more qualitative information about the design parameters were achieved. The results of this study show that the effects of the 2 investigated factors (thread height and width) on maximum EQV stress in jawbone are likely to be interrelated. The effect of these variables on maximum EQV stress in the jawbone cannot be analyzed independently. This is another important finding of the present study, because many previous finite element studies examined the effect of only 1 implant design parameter.[8,15] The conclusions of previous finite element studies should be reconsidered in light of these findings.

Model Design

The use of the FEM in implant biomechanics analysis offers many advantages over other methods in the simulation of complex clinical situations. However, because of simplifications intrinsic to FEM, several assumptions were made in the development of the model in the present study. The structures in the models were all assumed to be homogenous and isotropic and to possess linear elasticity. These are incorrect assumptions for, for instance, the living tissue modeled. Actual cortical bone of the mandible is transversely isotropic and inhomogeneous.[24] Hojjatie and Anusavice[25] also assumed that all materials were linearly elastic, homogeneous, and isotropic and ignored cement thickness in their finite-element stress analysis study. Cement thickness was also ignored in the current study because it does not affect the stress distribution.[26]

Zhou et al[27] concluded that expanding the domain of the model could reduce the effect of inaccurate modeling of the boundary conditions. This, however, is at the expense of computing and modeling time. Teixeira et al[28] concluded that in a 3D mandibular model (finite element analysis), modeling the mandible at distances greater than 4.2 mm mesially or distally from the implant did not result in any significant further yield in accuracy. Since simulation of the whole mandibular body is very elaborate, smaller models have been proposed for parameter studies.[29] In the present analysis, a segment of bone was modeled in an attempt to approximate the posterior region of the mandible. Since there is no guideline for the appropriate mesiodistal length of a mandibular segment for finite element analysis, a trial run comparing 2 lengths (36 mm and 18 mm) was performed for the models. Because of simplifications intrinsic to FEM, it is advisable to focus on qualitative rather than quantitative data from these analyses.[30] The results of the 2 models were qualitatively similar, and no difference in stress/strain tendencies was found between the 2 bone lengths. Thus, both models were considered suitable for this comparative analysis, and the results with the longer segment were reported in the present study.

Patra et al[31] reported that the anterior mandible is associated with 100% cortical osseointegration and that this percentage of cortical integration decreases toward the posterior region. The least cortical osseointegration (< 25%) is seen in the posterior maxilla. The degree of osseointegration appears to depend on bone quality and stresses developed during healing and function. In the present study, no debonding was allowed at the implant-bone interface. Other finite element analyses have shown remarkable differences in the values and sometimes even in the distributions of stresses between "fixed bond," "slip contact," and "nonlinear contact" interface boundary conditions.[15,32–35] It is unclear which interface boundary condition is most realistic; more experimental evidence is needed.[32] However, removal torque tests have shown higher scores for implants with rough (titanium dioxide–blasted or titanium plasma-sprayed) surfaces than for those with machined surfaces. The removal of rough-surfaced implants has frequently resulted in fractures in bone distant from the implant surface,[36] which suggests the existence of an implant-bone "bond." Since the present study simulated an osseointegrated screw-type implant with a rough surface, a "fixed bond" condition was set at its interface with bone as an approximation.

In studies of the entire mandible in which convergence tests with mesh refinements have been performed, models with more than 13,720 or 10,420 nodes showed convergent results.[37,38] A fine mesh is a major factor in the achievement of an accurate model. Thus, in the present study, only a mandibular segment with an extremely fine mesh around the implant (areas of high stress) was modeled (Fig 3). This resulted in models consisting of an average of 52,000 nodes, a number that was considered to ensure a sufficiently fine mesh for the given geometry. No further mesh refinement was performed.

It has been reported that even loads below the ultimate bone stress can cause bone failure, as in the case of fatigue failures, in which the microdamage of bone can no longer be repaired.[14] Accumulated microdamage may result in bone resorption. A study[39] also showed that threaded implants had higher remodeling rates and less mineralized bone formation when loaded with axial force than nonloaded threaded implants. These responses were triggered by tissue microdamage as a direct consequence of load application.[39] Functionally, there is always applied force acting on bone modified by an implant design, and there is always resisting force acting on the implant through the viscoelastic properties of the trabecular structure.[19,40] Through biomechanical events in bone, osseous tissue can be stimulated within physiologic limitations by implant design to develop along the lines of compressive forces dependent on the implant load-bearing area to sustain equilibrium.[18,31]

Bivariate Analyses

Based on the bivariate response surface (Figs 4 to 7) of the current study, as thread height and width decreased, Max EQV stress in cancellous bone increased by 63.0% under AX load. As thread height decreased and thread width increased, Max EQV stress in cancellous bone increased by 118.0% under 45-degree BL load. Increases for either type of load were much higher in cancellous bone than in cortical bone. This indicates that the effect of the 2 thread parameters on Max EQV stress is more significant in cancellous bone than in cortical bone. Under 45-degree BL load, the values of Max EQV stress in cortical and cancellous bone increased by 19.3% and 118.0%, respectively, and the value was much higher than under AX load. This indicates that the 45-degree BL load is apt to be influenced by the 2 thread parameters.

Univariate Analyses

According to the univariate analysis (single parameter) of Max EQV stress (Table 2), with decrease of the thread height, Max EQV stress in cancellous bone increased by 85.86% and 70.54% under AX and 45-degree BL load, respectively. Max EQV stress in cortical bone increased by 4.32% under AX load. The changes of Max EQV stresses in cortical bone were similar under 45-degree BL load with change of thread height or width. The results demonstrate that thread height affects the Max EQV stress of jawbone more than thread width under either AX or 45-degree BL load. Increased thread height favors improved stress distribution more in cancellous bone in comparison with cortical bone.

On the other hand, Max EQV stress in cancellous bone increased by 15.04% and 18.85% under AX and 45-BL loads, respectively, with variation of the thread width. Increased percentages were higher in cancellous bone than in cortical bone. This indicates that thread width has a greater impact on stress distribution in cancellous bone than in cortical bone.

Analysis of the tangent slope of the univariate response curves showed that stress (and variation of stress) in the cortical bone could be minimized when thread height ranged from 0.33 mm to 0.50 mm and width ranged from 0.18 mm to 0.30 mm. When the thread height exceeded 0.34 mm and width was less than 0.30 mm, the slightest variation of stress in cancellous bone could be achieved, and the minimal stress was found. Thus, thread heights of 0.34 mm to 0.50 mm and thread widths of 0.18 mm to 0.30 mm are optimal for a screw-type implant from a biomechanical point of view.

Sensitivity Analyses

Like the univariate analysis, the sensitivity analysis showed that thread height affected the Max EQV stress of the jawbone much more than thread width.

It indicates that thread height is much more important to the reduction of bone stress than thread width and that more attention should be paid to thread height than thread width for optimal design of screw-type implants from a biomechanical point of view.

CONCLUSIONS

Based on the results of these analyses, the following conclusions can be drawn regarding the effects of thread height and width on osseointegrated screw-type implants on stress distribution in the jawbone:

1. Stress in cancellous bone is apt to be influenced by thread parameters.
2. Force applied 45 degrees buccolingually is likely to be influenced by thread parameters.
3. Thread heights of 0.34 to 0.50 mm and thread

widths of 0.18 to 0.30 mm are optimal for screw-type implants from a biomechanical point of view.
4. More attention should be paid to thread height than to thread width in the design of screw-type implants.

REFERENCES

1. Cehreli M, Duyck J, De Cooman M, Puers R, Naert I. Implant design and interface force transfer. A photoelastic and strain-gauge analysis. Clin Oral Implants Res 2004;15:249–257.
2. Matsushita Y, Kitoh M, Mizuta K, Ikeda H, Suetsugu T. Two-dimensional FEM analysis of hydroxyapatite implants: Diameter effects on stress distribution. J Oral Implantol 1990;16:6–11.
3. Meijer HJA, Kuiper JH, Starmans FJM, Bosman F. Stress distribution around dental implants: Influence of superstructure, length of implants, and height of mandible. J Prosthet Dent 1992;68:96–102.
4. Palmer RM, Smith BJ, Palmer PJ, Floyd PD. A prospective study of Astra single tooth implants. Clin Oral Implants Res 1997;8:173–179.
5. Holmgren EP, Seckinger RJ, Kilgren LM, Mante F. Evaluating parameters of osseointegrated dental implants using finite element analysis—A 2-dimensional comparative study examining the effects of implant diameter, implant shape, and load direction. J Oral Implantol 1998;24:80–88.
6. Nordin T, Jönsson G, Nelvig P, Rasmusson L. The use of a conical fixture design for fixed partial dentures. A preliminary report. Clin Oral Implants Res 1998;9:343–347.
7. Norton MR. Marginal bone levels at single tooth implants with a conical fixture design. The influence of surface macro- and microstructure. Clin Oral Implants Res 1998;9:91–99.
8. Chun HJ, Cheong SY, Han JH, et al. Evaluation of design parameters of osseointegrated dental implants using finite element analysis. J Oral Rehabil 2002;29:565–574.
9. Tada S, Stegaroiu R, Kitamura E, Miyakawa O, Kusakari H. Influence of implant design and bone quality on stress/strain distribution in bone around implants: A 3-dimensional finite element analysis. Int J Oral Maxillofac Implants 2003;18:357–368.
10. Ivanoff CJ, Grondahl K, Sennerby L, Bergstrom C, Lekholm U. Influence of variations in implant diameters: A 3- to 5-year retrospective clinical report. Int J Oral Maxillofac Implants 1999;14:173–180.
11. Brunski JB. Biomechanical considerations in dental implant design. Int J Oral Implantol 1988;5:31–34.
12. Misch CE. Contemporary Implant Dentistry, ed 2. St. Louis: Mosby, 1999.
13. Bumgardner JD, Boring JG, Cooper RC Jr, et al. Preliminary evaluation of a new dental implant design in canine models. Implant Dent 2000;9:252–260.
14. Brånemark P-I, Hansson BO, Adell R, et al. Osseointegrated implants in the treatment of the edentulous jaw. Experience from a 10-year period. Scand J Plast Reconstr Surg 1977;16(suppl):1–132.
15. Hansson S, Werke M. The implant thread as a retention element in cortical bone: The effect of thread size and thread profile: A finite element study. J Biomech 2003;36:1247–1258.
16. Barbier L, Schepers E. Adaptive bone remodeling around oral implants under axial and nonaxial loading conditions in the dog mandible. Int J Oral Maxillofac Implants 1997;12:215–223.
17. Iplikcioglu H, Akca K. Comparative evaluation of the effect of diameter, length and number of implants supporting three-unit fixed partial prostheses on stress distribution in the bone. J Dent 2002;30:41–46.
18. Steigenga JT, al-Shammari KF, Nociti FH, Misch CE. Dental implant design and its relationship to long-term implant success. Implant Dent 2003;12:306–315.
19. Geng JP, Ma QS, Xu W, Tan KBC, Liu G. Finite element analysis of four thread-form configurations in a stepped screw implant. J Oral Rehabil 2004;31:233–239.
20. Zienkiewicz OC. The Finite Element Method in Engineering Science, ed 4. New York: McGraw-Hill, 1989.
21. Timoshenko SP, Goodier JN. Theory of Elasticity. Singapore: McGraw-Hill, 1984.
22. Kitamura E, Stegaroiu R, Nomura S, Osamu M. Biomechanical aspects of marginal bone resorption around osseointegrated implants: Considerations based on a three-dimensional finite element analysis. Clin Oral Implants Res 2004;15:401–412.
23. Kitamura E, Stegaroiu R, Nomura S, Miyakawa O. Influence of marginal bone resorption on stress around an implant;209;A 3-dimensional finite element analysis. J Oral Rehabil 2005;32:179–286.
24. Cochran DL. The scientific basis for clinical experiences with Straumann implants including the ITI dental implant system: A consensus report. Clin Oral Implants Res 2000;11:33–58.
25. Hojjatie B, Anusavice KS. Three dimensional finite element analyses of glass ceramic dental crowns. J Biomechanics 1990;23:1157–1166.
26. Matsushita Y, Kitah M, Mizuta K, Ikeda H, Suetsugu T. Two dimensional FEM analysis of hydroxyapatite implants: Diameter, effects on stress distribution. J Oral Implantol 1990;16:6–11.
27. Zhou X, Zhao Z, Zhao M, Fan Y. The boundary design of mandibular model by means of the three-dimensional finite element method. West China J Stomatol 1999;17:1–6.
28. Teixeira ER, Sato Y, Shindoi N. A comparative evaluation of mandibular finite element models with different lengths and elements for implant biomechanics. J Oral Rehabil 1998;25:299–303.
29. Meijer HJA, Starmans FJM, Bosman F, Steen WHA. A comparison of three finite element models of an edentulous mandible provided with implants. J Oral Rehabil 1993;20:147–157.
30. Iplikcioglu H, Akca K. Comparative evaluation of the effect of diameter, length and number of implants supporting three-unit fixed partial prostheses on stress distribution in the bone. J Dent 2002;30:41–46.
31. Patra AK, DePaolo JM, D'Souza KS, DeTolla D, Meenaghan MA. Guidelines for analysis and redesign of dental implants. Implant Dent 1998;7:355–368.
32. Brunski JB. Biomechanical factors affecting the bone-dental implant interface. Clin Mater 1992;10:153–201.
33. Brunski JB. In vivo response to biomechanical loading at the bone/ dental-implant interface. Adv Dent Res 1999;13:99–119.
34. Van Oosterwyck H, Duyck J , Vander Sloten J, et al. The influence of bone mechanical properties and implant fixation upon bone loading around oral implants. Clin Oral Implants Res 1998;9:407–418.
35. Duyck J, Naert I, Rønold HJ, Ellingsen JE, Van Oosterwyck H, Vander Sloten J .The influence of static and dynamic loading on marginal bone reactions around osseointegrated implants: An animal experimental study. Clin Oral Implants Res 2001;12:207–218.
36. Gotfredsen K, Berglundh T, Lindhe J. Anchorage of titanium implants with different surface characteristics: An experimental study in rabbits. Clin Implant Dent Relat Res 2000;2:120–128.

37. Chen J, Lu X, Paydar N, Akay HU, Roberts WE. Mechanical simulation of the human mandible with and without an endosseous implant. Med Eng Phys 1994;16:53–61.
38. Hart RT, Hennebel VV, Thongpreda N, van Buskirk WC, Anderson RC. Three-dimensional finite element study of the biomechanics of the mandible. J Biomech 1992;25:261–286.
39. Hoshaw SJ, Brunski JB, Cochran GVB. Mechanical loading of Brånemark implants affects interfacial bone modeling and remodeling. Int J Oral Maxillofac Implants 1994;9:345–360.
40. Strong JT, Misch CE, Bidez MW, Nalluri P. Functional surface area: Thread-form parameter optimization for implant body design. Compend Contin Educ Dent 1998;19:4–9.
41. Cook SD, Klawitter JJ, Weinstein AM. A model for the implant-bone interface characteristics of porous dental implants. J Dent Res 1982;61:1006–1009.
42. Borchers L, Reichart P. Three-dimensional stress distribution around a dental implant at different stages of interface development. J Dent Res 1983;62:155–159.
43. Colling EW. The Physical Metallurgy of Titanium Alloys. Metals Park, OH: American Society for Metals, 1984.
44. Lewinstein I, Banks-Sills L, Eliasi R. Finite element analysis of a new system (IL) for supporting an implant-retained cantilever prosthesis. Int J Oral Maxillofac Implants 1995;10:355–366.